NeuroImage 48 (2009) 532–540

Contents lists available at ScienceDirect

NeuroImage

journal homepage: www.elsevier.com/locate/ynimg

Combinatorial fiber-tracking of the human brain

Shlomi Lifshits [a,b], Arie Tamir [c], Yaniv Assaf [a,b,*]

[a] Department of Neurobiology, Faculty of Life Sciences, Tel Aviv University, Tel Aviv, Israel
[b] Functional Brain Imaging Unit, The Wohl Institute for Advanced Imaging, Tel Aviv Sourasky Medical Center, Tel Aviv, Israel
[c] Department of Statistics and Operations Research, School of Mathematical Sciences, Tel Aviv University, Israel

ARTICLE INFO

Article history:
Received 30 June 2008
Revised 27 April 2009
Accepted 26 May 2009
Available online 6 June 2009

ABSTRACT

This paper presents a novel fiber-tracking algorithm, termed combinatorial tracking, which uses stochastic process modeling and global optimization algorithm for tractography. Combinatorial tracking is a probabilistic tracking algorithm that transforms the brain's white matter into a grid in which each voxel has 26 weighted connections with adjacent voxels. We model the random walk on this graph using a Markov Chain model and suggest two approaches for fiber reconstruction. In the first approach, we find the most probable paths between two voxels with prior connectivity knowledge using a shortest path algorithm. In the second approach, the all-pairs mean first passage time (MFPT) matrix **M** (or hitting time as referred to in the Spectral Graph theory literature) is calculated analytically. We suggest that **M** can be interpreted as a global connectivity matrix and use it for fiber reconstruction. We also introduce a simulation framework that can be used to calculate specific elements of the matrix **M**, and show how it can be employed to select the target of a fiber in a high resolution diffusion tensor imaging (DTI) dataset.

Because any source and any target voxel can be connected, combinatorial tracking permits true connectivity analysis, overcoming the limitations of conventional tracking, especially stopping criteria (e.g. low FA).

We applied combinatorial tracking to a standard DTI dataset and demonstrated the reconstruction of the cortico-thalamic pathway, the pyramidal decussation, and the medial cerebellar peduncle fibers. While the DTI ellipsoid served as input for the algorithms, any diffusion imaging based orientation density function (ODF) can be used. This framework can potentially turn diffusion imaging tractography into a true connectivity measure.

© 2009 Elsevier Inc. All rights reserved.

Introduction

Tractography – an application of diffusion tensor imaging – has been used in recent years for the analysis of fiber pathways and brain connectivity indices (Basser et al., 2000; Mori et al., 1999; Conturo et al., 1999; Catani et al., 2002; Behrens et al., 2003a; Ciccarelli et al., 2006; Jbabdi et al., 2007). Common DTI-based tractography algorithms reconstruct a fiber by following the direction pointed by the diffusion tensor's largest eigen-vectors (assumed to represent the main direction of the fibers within a voxel) from a seed region of interest (ROI) (Basser et al., 2000; Mori et al., 1999). These types of algorithms successfully segment the white matter into anatomically known fiber fascicles or pathways (Catani et al., 2002). Clinical applications of such an approach have ranged from the mapping of white matter systems prior to surgical intervention to the estimation of white matter aberrations in developmental disorders, neurological diseases and psychiatric disorders (Rollins, 2007; Price et al., 2008; Schonberg et al., 2006; Huppi and Dubois, 2006; Mukherjee, 2005; Mukherjee and McKinstry, 2006; Witwer et al., 2002; Ge et al., 2005; Assaf et al., 2006; Assaf and Pasternak, 2008).

Fiber-tracking suffers from several problems, some related to the inherent DTI analysis limitations and others to the tractography analysis routine: 1) crossing fibers — DTI analysis assumes that each voxel contains a single population of neuronal fibers and thus calculates an artifactual fiber orientation estimation in voxels containing two or more fiber orientations (Assaf and Pasternak, 2008; Pierpaoli et al., 1996); 2) partial volume effect — as DTI averages the contribution from all compartments, voxels that contain CSF or gray matter might be excluded from the reconstructed path due to low fractional anisotropy (FA) (Chou et al., 2005; Papadakis et al., 2002; Alexander et al., 2001); 3) seed ROI — the selection of the seed ROI has a tremendous impact on the resulting track (Schonberg et al., 2006); 4) largest eigen-value uncertainty due to noise (either physiological or scanner based) might lead to an artifactual reconstructed fiber (Jones, 2003); and 5) ground truth validation (Dyrby et al., 2007) — in contrast to the extensively studied gray matter, the 3D arrangement of the white matter and its fascicle organization has been

* Corresponding author. Department of Neurobiology, Faculty of Life Sciences, Tel Aviv University, Tel Aviv, 69978, Israel. Fax: +972 3 6407168.
E-mail address: asafyan@zahav.net.il (Y. Assaf).

1053-8119/$ – see front matter © 2009 Elsevier Inc. All rights reserved.
doi:10.1016/j.neuroimage.2009.05.086

studied less and the location of each path can only be roughly estimated; this lack of ground truth precludes comparisons between tracking algorithms.

It was suggested recently that probabilistic tracking has the potential to overcome some of the limitations of classical tractography (Behrens et al., 2003a; Jbabdi et al., 2007; Jones and Pierpaoli, 2005; Lazar and Alexander, 2005; Koch et al., 2002; Poynton et al., 2005; Parker et al., 2003; Behrens et al., 2003b; Zhang et al., 2009). The probabilistic approach has advantages over classical tractography: 1) it can employ advanced diffusion models for fiber-tracking (models that address the issue of crossing fibers and partial volume effect); 2) artifactual tracts caused by the deviation of the fiber due to large uncertainty in the eigen-vector can be eliminated by assigning them low probability and excluding them; and 3) it allows quantitative measurement of 3D connectivity.

Combinatorial tracking follows the general concept of probabilistic tracking. The brain is transformed into a grid in which each voxel has 26 weighted connections with adjacent voxels. When weights are assigned transition probabilities (computed from DTI data), the model is transformed to a Markov Chain model (random walk on a weighted graph). From the Markov chain transition probability matrix **P**, the all-pairs MFPT matrix **M** (or hitting time, as referred to in the Spectral Graph theory literature (Chung, 1997)) is calculated analytically and interpreted as a global connectivity matrix. We propose two tracking algorithms based on **P** and **M**, both of which require prior knowledge of the gray matter origin and the target of a fiber: 1) the most probable random walk path (MP); and 2) the reaction path algorithm (RP). We also introduce a simulation method, termed target selection by simulation (TSS), which enables the calculation of specific elements of the matrix **M**, and show how it can be employed to select the target of a fiber in a high resolution DTI dataset. The algorithms are described below in the Theory section, followed by a brief description in the Materials and methods section of the pre-processing routine of our DTI dataset before it was used as input to the combinatorial tracking framework. The Results section presents the execution of the two algorithms on synthetic data, and the results of applying them to the reconstruction of different parts of the motor pathway. The Discussion covers the advantages and disadvantages of combinatorial tracking as well as the differences between its algorithms.

Theory

The algorithm flow diagram is presented in Fig. 1a. In the model construction phase, the Markov chain transition probability matrix **P** is calculated by discretization of the diffusion tensor field as calculated by the DTI. Then, the all-pairs MFPT matrix **M** is calculated from **P** by a linear algebraic method. Two fiber-tracking algorithms are introduced: the MP algorithm, which solves a shortest path problem on the graph with transformed weights, and the RP algorithm, which reconstructs a path by finding a path from source to target with minimum number of edges among all paths with a decreasing MFPT to the target.

It should be noted that the input for the algorithm was the DTI analysis output (i.e. diffusion ellipsoid), but any orientation density function can be used.

Spatial discretization

For each voxel, the 3D space is divided into 26 regions, each centered by the direction from the center of the voxel to the center of a neighboring voxel. Diffusion is assumed to occur from a point at the center of the voxel. The displacement probability density function (PDF) is modeled by a tri-variate Gaussian distribution whose variance–covariance matrix is proportional to the diffusion tensor **D** (calculated from conventional DTI analysis, see Materials and methods) and diffusion time t (Eq. (1)).

$$P_i(\boldsymbol{X},t) = \frac{1}{\sqrt{(2\pi)^3\,|2D_it|}} e^{\left(-\frac{1}{2}\boldsymbol{X}'(2D_it)^{-1}\boldsymbol{X}\right)} \quad (1)$$

where $\boldsymbol{X}$ is a 3D displacement vector, D_i is the diffusion tensor measured at voxel i, and $P_i(\boldsymbol{X},t)$ is the value of the PDF of voxel i, for a

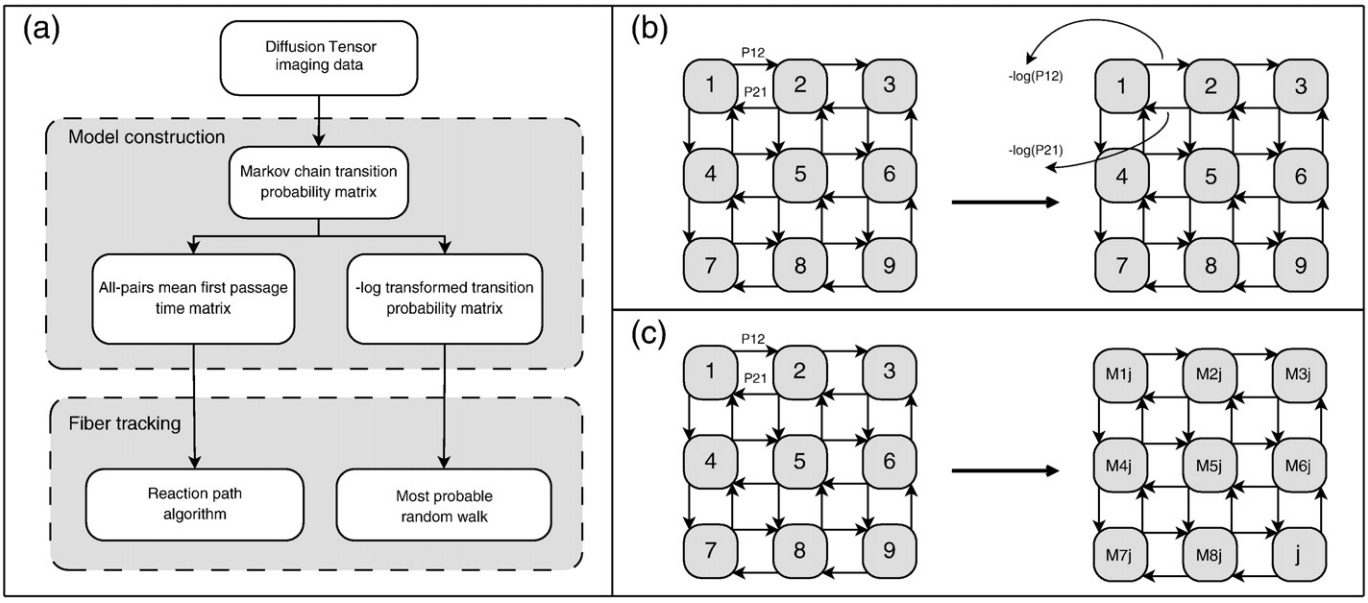

Fig. 1. Combinatorial tracking analysis steps: (a) starting with a DTI dataset, a Markov chain model is constructed by discretization. Two fiber-tracking algorithms are introduced, one based on the transformed transition probability matrix **P** and the other on the all-pairs MFPT matrix **M**. (b) The network model is transformed by applying the −log transformation on the edges weights, which reduces the maximum probability path problem to a shortest path problem with non-negative weights. (c) By calculating the all-pairs MFPT matrix **M**, we transform the model from a network model, where the information lies on the edges, to a network model, where the information lies in the nodes. The M_{ij} values on the network on the right scores the connectivity level of each network node to the node j.

displacement $\boldsymbol{X}$ and time t. By substituting $t=1/2$ in Eq. (1), displacement samples can be generated by drawing from a tri-variate Gaussian distribution with variance–covariance matrix $\mathbf{D}$ (we experimented with several diffusion times and found no difference in results, so we used $t=1/2$ for simplicity). These samples are used in a Monte-Carlo scheme for the estimation of p_{ij}, the probability that a particle, initially located at the center of voxel i, is found in the region directed at the neighbor j after $t=1/2$ s.

The Monte-Carlo scheme involves the classification of a sample from a tri-variate Gaussian distribution to one of 26 regions. The classification is performed by the Minimal Angle method (Fig. 2): a sample (x,y,z) is classified to a region if the angle it creates with the vector $\boldsymbol{v}$ (pointing at a neighbor voxel center) is minimal among all other angles. Since the method classifies each sample to a unique region, it implicitly partitions the 3D space (Fig. 3).

The estimated probability p_{ij} is calculated as the proportion of samples that are classified to a region j. We further averaged the estimators for the two opposite directions in order to increase the estimation precision.

Network model

The white matter is modeled as a network, where the center of each voxel is mapped to a vertex and each vertex i is connected to its 26 neighbors j by directed edges which are assigned probabilities p_{ij}. In the network construction process, a voxel is connected to its neighboring voxels in the white matter, but not to voxels outside the white matter. In the case where a voxel has non-white matter neighbors, we correct the probabilities by normalization such that $\sum_i p_{ij} = 1$.

The process results in a set of strongly connected components where every component is interconnected by a set of bi-directional edges. We further extract the largest, strongest connected component. The construction scheme results in a graph that corresponds to a finite state discrete time irreducible Markov Chain model (see Appendix A).

Fiber reconstruction using most probable random walk (MP) path

There have been several attempts to solve global combinatorial optimization problems on the white matter graph constructed from DTI data. Poynton et al. (2005) also used the tri-variate Gaussian PDF model. An edge weight was assigned the value of Eq. (1) where $\boldsymbol{X}$ is the distance between the adjacent voxel centers. The problem was thus reduced to a shortest path problem and was solved by dynamic programming. Iturria-Medina et al. (2007) constructed a weighted non-directed graph for the brain (white matter and gray matter). A weight was assigned to each edge, indicating the probability that a fiber connection between the adjacent voxels exists. They solved the most probable path between two nodes by defining the optimal path between nodes i and j as the path that maximizes the product of the conditioned probabilities along the path. The conditioned probability in this case was the probability of the events "edge E_{jk} exists provided that E_{ij} exists". The edge existence probability $P(E_{ij})$ was computed by combining the result of the integration of the ODF of voxel i over a cone directed at voxel j with the result of the integration the ODF of voxel j over a cone directed at voxel i and the probability that voxels i,j are in fact white matter voxels. They also introduced a curvature regularization term. Fout and Huang (2005) calculated a "connection probability" for every pair of neighboring voxels according to the neighbor's PDF and the application of Bayes rule. Then they used these probabilities as edge weights. They found the maximum path with n edges (where n is a parameter) using dynamic programming. As a post-processing step, they reconstructed a biological smooth path guided by the optimal path. Sherbondy et al. (2008) described a method for finding the most probable track between brain areas that are known to be connected, a situation that frequently arises in the visual system. First, candidate paths were collected by a search algorithm that originated from the selected origin and target ROIs. Second, each path was scored according to the diffusion tensors, which were measured along the path, and the geometrical features of the path. Then, the most probable path was selected. The algorithm is probabilistic in the sense that the path score is in fact a posterior probability: that is, the product $\mathrm{p}(D|s)\mathrm{p}(s)$, where $\mathrm{p}(D|s)$ is the likelihood of measuring such diffusion tensors given that the path is s. $\mathrm{p}(s)$ is a prior for the existence of a path with geometrical features as in s. It is probabilistic also because the path collection algorithm draws a step direction from the Watson distribution.

Our MP algorithm reconstructs a path in the white matter (with known origin and target) using the Markov Chain model by solving a global combinatorial optimization problem: given that a state sequence starts at state i and ends at state j, find the sequence of states that starts at i and ends at j (with no repeating states), with maximum probability. The optimal path is a simple path from the source to the target, which maximizes the product of transition probabilities along its edges. We use an equivalent optimization problem: find the path from source to the target that minimizes the sum of $-\log$ of the transition probabilities along its edges. By using the equivalent optimization problem, we reduce the problem of

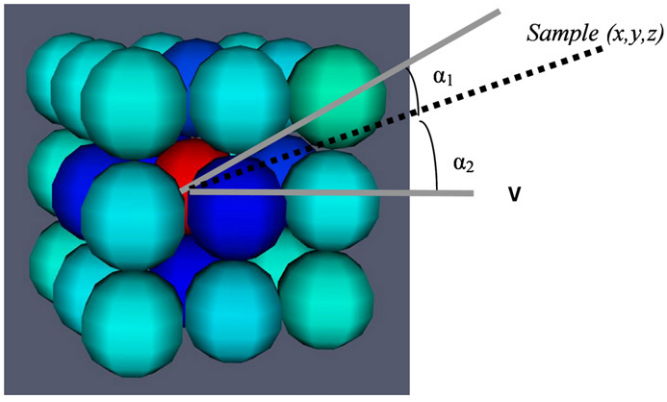

Fig. 2. The Minimal Angle method: in the discretization process, samples (3D vector) are drawn from a tri-variate Gaussian distribution. The angle formed by the sample with the different members of the neighborhood is calculated (for example α_1, α_2). The sample is classified to the neighbor with the smallest angle. The voxels are represented by spheres, where the red sphere is the voxels for which the sample (x,y,z) is generated.

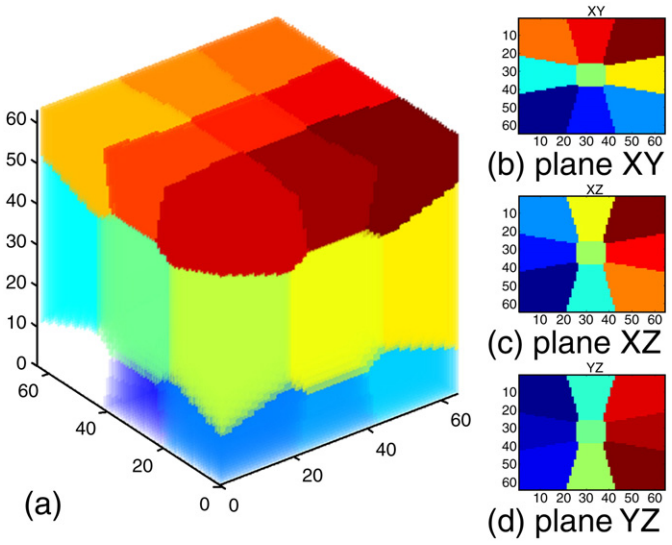

Fig. 3. Discretization of the tensor field: classification of points in a neighborhood using the minimal angle method. Points in the neighborhood of a voxel whose dimensions are a ratio of 1:1:1 are classified using the minimal angle method. Neighbor classification is indicated by different colors. In (b)–(d), different planes of the neighborhood are displayed, showing the symmetry of this sectioning method.

finding a maximum probability path to a problem of finding a shortest path in a graph with non-negative weights. In order to solve the optimization problem, the graph adjacency matrix is applied to the transformation $-\log(p_{ij})$ (Fig. 1b), and the shortest path is found by applying Dijkstra's shortest path algorithm (Ahuja et al., 1993).

The algorithm was implemented in Matlab (MathWorks, MA, USA) using BGL (2002) and Matlab BGL interface (David Gleich, Stanford University).

Fiber reconstruction using reaction path (RP) algorithm

In Markov Chains theory, the first passage time *Vy* is defined as the time until first arrival to state *y* when starting at a specific state *V*. We denote M_{ij} as the expected value of the first passage time (mean first passage time, MFPT) from state *i* to state *j*. Note that MFPT is equivalent to the term Hitting time in the Spectral Graph theory literature (Chung, 1997). Since the Markov Chain is finite and irreducible, the all-pairs MFPT matrix can be calculated by applying the fundamental matrix theorem (Grinstead and Snell, 1997), preceded by calculation of the stationary distribution using the GTH (Grassmann et al., 1985) algorithm (see Appendix A). The calculation involves finding the inverse of a large matrix: for example, for a volume of $64\times64\times28$ voxels the resulting chain has about 10,000 states, and the calculation of the all-pairs MFPT matrix requires finding the inverse of a 10,000 by 10,000 matrix. The inverse matrix is found by first applying the LU decomposition using ATLAS (Whaley and Dongarra, 1998) (single precision floating point).

We suggest that the MFPT from *i* to *j* M_{ij} scores the connectivity level of *i* to *j* as it is affected by the probability of every path from *i* to *j*; thus, it is a natural measure of connectivity in the white matter network. Note that in contrast to the transition probability, which is a characteristic of an edge, M_{ij} is a characteristic of a node for a specific target *j* (Fig. 1c).

The reaction path (RP) algorithm finds a minimum length path (in number of edges) from *i* to *j* among all paths that start at *i* and decrease the MFPT to the target voxel *j*. The algorithm follows Park et al.'s (2003) method for calculating a chemical reaction path. In many chemical and biological reactions, initial and final states are known but reaction pathways connecting the two are not. Park denotes the MFPT from state *x* to the product as $\tau(x)$, and uses it as a distance measure to the product. Once the MFPT $\tau(x)$ is determined for all states, the reaction path is constructed by following the direction along which τ decreases more rapidly (a next state is chosen from all possible states, such that the decrease in MFPT per distance is maximized).

Before the RP algorithm is applied, the **M** matrix is averaged ($M_{ij} \leftarrow (M_{ij}+M_{ji})/2$), resulting in a symmetric matrix (half of the Commute time as referred to in the Spectral Graph theory literature (Chung, 1997). An auxiliary network is then built by excluding all the edges that, when traversed, do not reduce the MFPT to the target; that is, all edges e_{kl} for which $(M_{lj}-M_{kj})>0$. Finally, the auxiliary network is searched for the shortest path (in number of edges) using the Breadth-first search (BFS) algorithm (Ahuja et al., 1993).

Target selection by simulation

We hypothesize that the target of a fiber can be selected from a candidate set by the minimum MFPT criterion. For cases in which the **M** matrix cannot be computed analytically because of its size, we introduce a statistical simulation method based on this assumption: target selection by simulation (TSS). TSS uses simulation to statistically estimate the M_{ij} values for every one of the fiber target candidates. For every target voxel, the algorithm selects a random source from the source set and starts 1000 random walks. In each iteration, the algorithm draws a next neighbor state from the probability mass function (by the inversion method with binary search). When the target is reached, the arrival time (number of iterations) is recorded. The algorithm stops when either 95% of the walkers have arrived at the target or a maximum of 1,000,000 iterations is exceeded. For the statistical estimation, we assume that the arrival time is distributed by the Gamma distribution. The expected value is estimated by the maximum likelihood estimation with censoring using Matlab. The censoring incorporates into the likelihood function the information that, although the arrival time of some random walkers is not known at the time the simulation was stopped, it is known that the arrival time is later than the stopping time. The algorithm returns the voxel with the minimum estimated arrival time among target candidates. After the target is selected, the path from the source can be reconstructed by applying by the MP algorithm (since we do not calculate the MFPT from all voxels to the target, the RP algorithm cannot be applied).

Materials and methods

MRI acquisition

The combinatorial tracking framework was implemented on conventional DTI datasets from two healthy subjects scanned on a 3 T GE scanner. The first DTI dataset consisted of 27 axial slices with resolution of $3.4\times3.4\times4.0$ mm^3, and the second consisted of 50 axial slices with resolution of $2.5\times2.5\times2.5$ mm^3. The scanning parameters were as follows: TE = 88 ms, b value of 1000 s/mm^2 (Δ/δ of 25/19 ms) acquired over 19 gradient directions. The acquisition was gated to 30 R–R cardiac cycles.

In addition to the DTI dataset, the acquisition included a T1-weighted spoiled gradient recalled echo (SPGR) experiment with the following parameters: 66 axial slices, TR/TE = 400/3.2 ms, and resolution $1\times1\times2$ mm^3.

DTI image analysis

Prior to DTI analysis, a correction of head motion image artifacts and normalization to Montreal Neurological Institute template (MNI) coordinate system was performed using the SPM software (version 2, UCL, London, UK). Correction of head motion image artifacts was performed using the least squares algorithm and a 6-parameter (rigid body) transformation. Each gradient direction volume of a DTI dataset also underwent spatial normalization using a 12-parameter affine non-linear transformation to MNI. The gradient directions were recalculated following the realignment and normalization procedures. DTI was analyzed with in-house software written in Matlab, which calculated the eigen-values, eigen-vectors, FA and ADC for each voxel, as described previously (Basser and Pierpaoli, 1998).

Generation of masks

Following DTI analysis, the SPGR dataset was used to create masks of the gray matter and white matter. The SPGR dataset was first normalized to the same MNI template as the DTI dataset. Following normalization, the SPM software was used to segment the brain to its white matter, gray matter and CSF components. In addition, the Talairach atlas was used to identify the location of the thalamus, the ventral posterior lateral nucleus (VPL) of the thalamus, and the M1/S1 cortical strip. The Talairach coordinates of the ROIs were transformed to MNI space using Matlab code written by Lauren R. Moo (Massachusetts General Hospital, Boston, MA, USA).

Results

Validation on synthetic data

The synthetic DTI data was generated by the "tend" application (Kindlmann[1]). The helix is illustrated in Fig. 4a by Box glyphs, where each diffusion tensor is represented by a box. Fig. 4b shows the Graph, which is constructed by first segmenting the helix from its surrounding and applying the discretization process described above. The results obtained with the MP and RP algorithms are shown in Figs. 4b and c, respectively, where the source and target were selected at each side of the helix. As can be seen, the tract follows the shape of the helix.

[1] Kindlmann, G. Brain dataset courtesy of Gordon Kindlmann at the Scientific Computing and Imaging Institute, University of Utah, and Andrew Alexander, W. M. Keck Laboratory for Functional Brain Imaging and Behavior, University of Wisconsin-Madison.

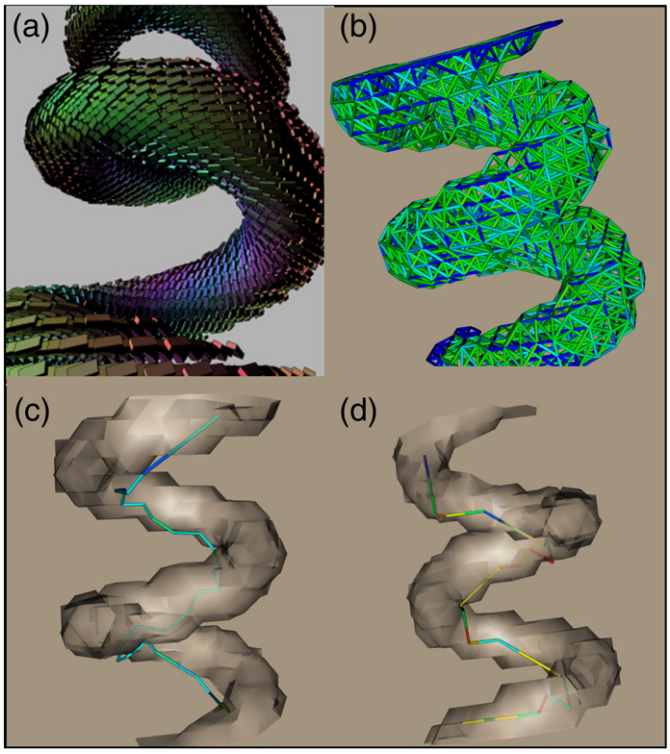

Fig. 4. Synthetic data: (a) a synthetic helical fiber. Diffusion tensors are displayed by Box glyphs. (b) The helix graph. Edges are colored according to transition probabilities. (c) Application of the MP algorithm to the helical fiber. Edges are colored according to transition probability. The gray iso-surface represents the area of high FA. (d) Application of the RP algorithm to the helical fiber. Edge color indicates the decrease in MFPT to the target.

Application to a brain DTI dataset

The different analyses that constitute the combinatorial tracking framework (as given in Fig. 1a) were applied on various segments of the motor pathway.

The MP algorithm was applied to reconstruct the cortico-thalamic pathway. The entire M1/S1 cortex was taken as a source region and the entire thalamus was taken as the target. As seen in Fig. 5, the most probable pathway proceeds towards the thalamus and enters lateral to it. This is consistent with other known anatomical pathways of this system. The MP also reconstructed the fanning of fibers into the cortex, which is also consistent with known anatomical appearances of this fiber system. It should be noted that conventional tracking algorithms often cannot reconstruct the entire fiber fanning due to crossing fiber artifacts. In addition a small fraction of the fibers enters the thalamus from its medial part and may appear as an artifactual pathway.

Fig. 6 compares the two different fiber reconstruction algorithms of combinatorial tracking: MP (Figs. 6a and c) and RP (Figs. 6b and d). We used each of the algorithms to reconstruct the pyramidal decussation (Figs. 6a and b) and the medial cerebellar peduncle fibers (Figs. 6c and d). These two fiber systems cross each other at the pons, posing in a complicated fiber system for reconstruction. For the pyramidal decussation, the source and target ROIs were placed at the cerebral peduncle and the medulla. For the medial cerebellar peduncle fibers, the ROIs were placed at the two ends of this system in the cerebellum. The medial cerebellar peduncle fibers were best reconstructed with the RP algorithms, while the MP algorithm found additional artifactual fibers connecting the source and target ROIs from an artifactual path.

In Fig. 7 the TSS algorithm is used to find the area on the thalamus that is connected to the M1/S1 cortex. In this analysis the source (the

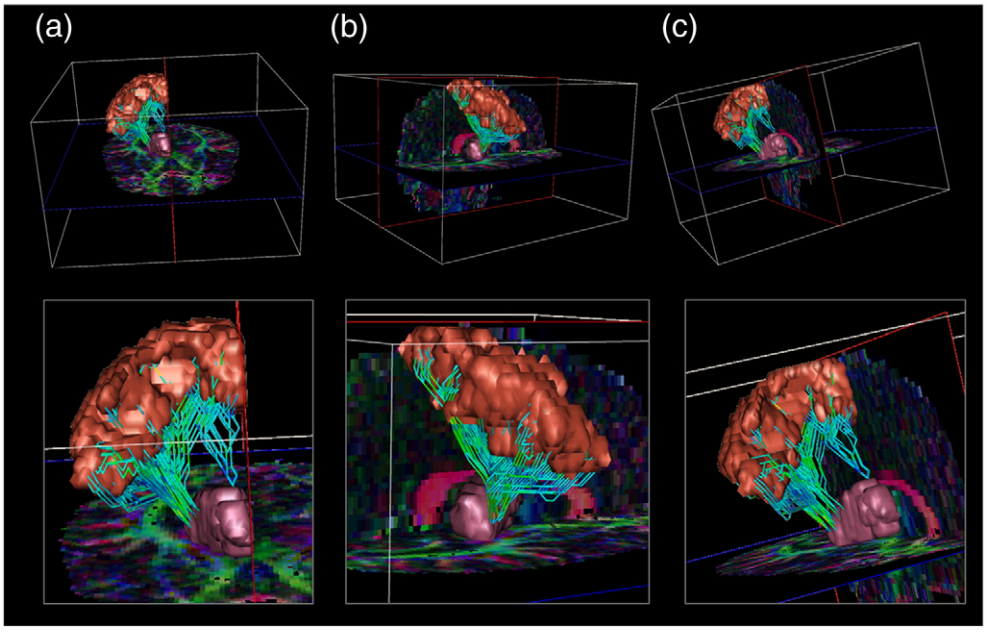

Fig. 5. Application of the MP tracking algorithm to the cortico-thalamic pathway: three views (a — front, b — medial, c — rear) of the cortico-thalamic pathway reconstructed using the MP algorithm. Each voxel in the M1/S1 cortex (bronze volume) was used as a source while each voxel in the thalamus (pink volume) was used as a target. Most of the fibers enter the thalamus at its lateral side in close proximity to the ventral posterior lateral (VPL) nuclei location. Note that the MP was able to reconstruct the fiber system including the fan-like appearance of fibers as they approach the cortex.

M1/S1 cortex) was divided into 17 segments, roughly resembling the homunculus mapping of the cortex. The target voxel on the thalamus was selected from each segment. Out of computational considerations, the analysis was done in two steps. First, the MFPT from the entire M1/S1 cortex to voxels on the shell of the thalamus was estimated. Low MFPT voxels on the thalamus were identified and passed to the second phase, where the MFPT was estimated from every segment of the M1/S1 cortex. Figs. 7a–c depict the cortical segment volumes (in different colors) and the thalamus (in pink), as well as the reconstructed fibers between every segment to the thalamus. Fig. 7d gives a closer look at the thalamus region where each voxel that has been selected as a target candidate in the first step is depicted by a sphere whose color encodes the mean MFPT from the M1/S1 cortex segments. The red sphere has the lowest MFPT and the blue spheres the highest. The ventral posterior lateral (VPL) nucleus of the thalamus is the anatomical target region of the cortico-thalamic

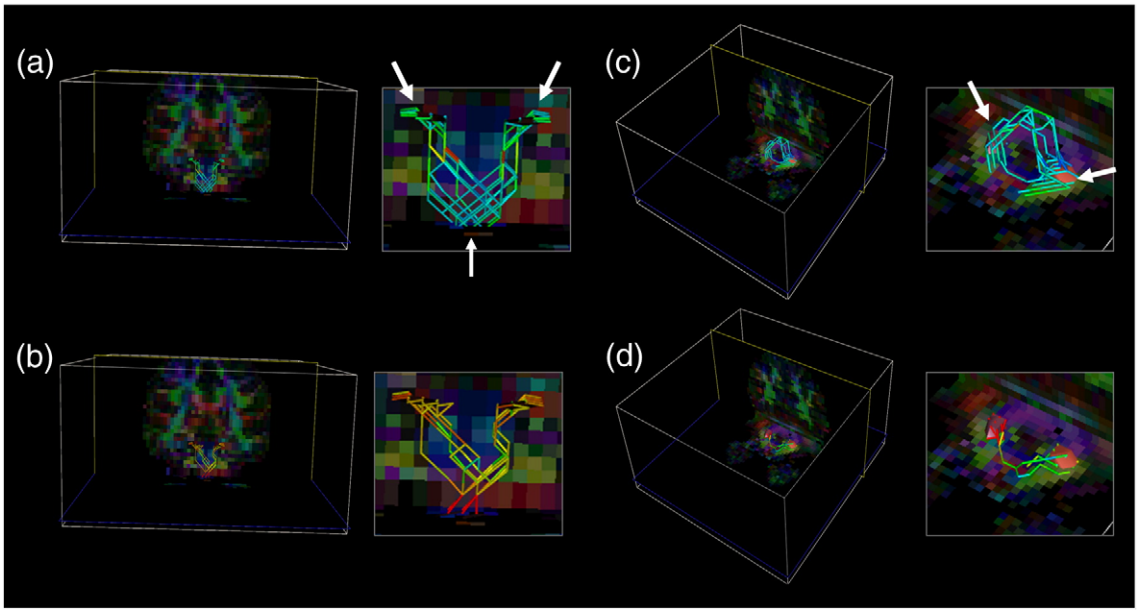

Fig. 6. Tracking of the pyramidal decussation and the medial cerebellar peduncle connections: the pyramidal decussation and cerebellar-pontine fibers were reconstructed with each of the two suggested algorithms for fiber-tracking (MP, RP). The ROIs are indicated by the red-orange volumes as well as by white arrows in a and c. (a) and (b) represent the tracking of the pyramidal decussation with MP and RP, respectively. (c) and (d) represent the tracking of the cerebellar-pontine fibers with MP and RP, respectively. Note that only (d) reconstructed the fiber system with good anatomical correspondence.

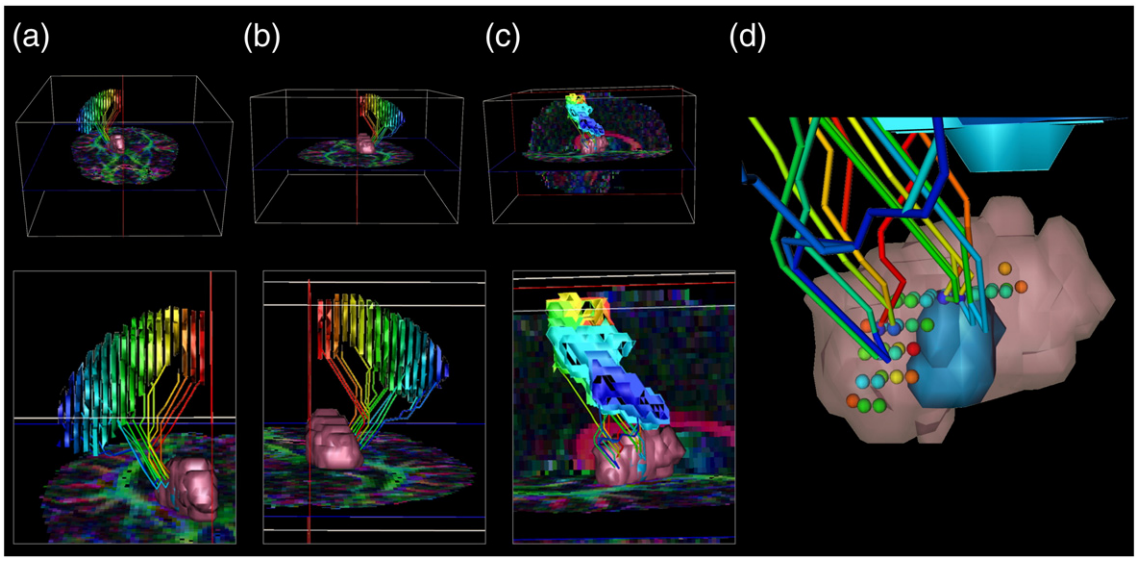

Fig. 7. Cortical-thalamus target selection: the same as in Fig. 5, but here the cortex was segmented into 17 segments, roughly resembling the homunculus, each assigned a different color from red to blue. From each segment TSS was used to find the most probable voxel target on the thalamus (pink) (d). Once the target was chosen, the corresponding cortical segment and target voxel could be connected using the MP algorithm (a–c). The voxels chosen as targets are indicated in (d) as spheres. The red sphere has the lowest MFPT. The blue volume represents the ventral posterior lateral (VPL) nucleus of the thalamus extracted from the Talairach atlas. Note the close proximity of the lowest MFPT spheres to the VPL volume.

fibers; its atlas location is marked by the blue volume. Note the close proximity of the selected target voxel spheres to the VPL atlas location. The fact that they do not coincide might be due to subject-atlas variability.

Discussion

The MP and RP algorithms are tracking algorithms in the sense that they find the white matter path that is most likely to connect two regions. The main difference between them and conventional fiber-tracking is the selection of the seed ROI. Conventional tracking requires defining a seed ROI from which tracks will be launched, such that it lies within the desired fiber system. The seed ROI selection procedure is subjective and prone to errors as it necessitates anatomical expertise and pre-knowledge of the 3D alignment and position of fiber tracks. The combinatorial tracking approach presented here enables defining the cortical regions that need to be connected and searching for the nearest white matter region to start the tractography. Thus, this approach is much more objective and, as demonstrated here, reproduces the anatomy with good correspondence.

The combinatorial tracking approach ensures objective connectivity analysis with diffusion imaging data. It is difficult to determine whether this or one of the other probabilistic approaches is superior since the ground truth of brain connectivity is unknown. But, the fact that combinatorial tracking can use a cortical source and target inputs elevates the DTI-based tractography from a plain fiber-tracking tool to a connectivity analysis method.

The synthetic data validated both the strengths and the limitations of the algorithms: both reconstructed the path but both required pre-segmentation of the white matter.

One of the main problems in fiber-tracking is how to deal with partial volume effect, such as crossing fibers. Crossing fibers within a pixel will lower the transition probabilities in the directions of the fibers, and the transition probability will be more uniform across neighbors. This may influence the probability of paths, but it is argued that the “true” path will still have higher probability than others, even with the regional effect of crossing fibers.

Differences between the tracking algorithms

The MP and the RP algorithms both start with source and target voxels, but they tackle tracking from different angles: the former finds a path by maximizing the product of probabilities, while the latter uses the MFPT to reconstruct a path. Because the search is performed on a strongly connected component of the graph, a path exists between every pair of voxels, which guarantees that the MP will find a path, though not a unique one. The path existence problem in the RP algorithm requires further exploration. Both algorithms tend to select shorter paths over longer paths (a path length is defined by the number of edges in it). Both algorithms are sensitive to isotropic environment; fiber reconstruction on the synthetic helical fiber showed that white matter pre-segmentation is a condition for successful reconstruction, and that when skipped, paths tend to penetrate the gray matter. The RP algorithms require calculating the all-pairs MFPT matrix, which involves calculating the inverse of a huge matrix, while the MP algorithm is solved in a very fast combinatorial optimization algorithm.

The TSS method

This approach should be used when the exact target voxel is unknown. It is a true connectivity analysis in which one defines a source and uses the algorithm to define the target(s) and the path that connects the source to the target(s). However, selection of the target by simulation might present a computational challenge. For example, estimating the MFPT to one voxel on the thalamus surface involves 100,000 simulation iterations, where each and every iteration involves drawing from a probability mass. Applying aliasing methods for drawing from a probability mass function may improve the algorithm performance.

Application of combinatorial tracking

We first tested combinatorial tracking on the thalamus and the M1/S1 strip of the cortex as source and target regions. The MP approach reconstructed this fiber system in an anatomically consistent manner, producing the fan-like structure of fiber that originates

from the thalamus and fans into the cortex. Conventional tracking algorithms find only part of the fiber fanning because of their ending criteria: because the FA drops to below 0.2 along the path of the fan (its lateral parts) due to intersection with other fiber systems, conventional tracking algorithms stop at the middle of the path and most fibers reach only a small section of the M1/S1 strip. With combinatorial tracking, a source and target voxel must be connected, even if the probability is low at some part of the path.

The TSS method enabled us to identify the target of fibers that start from the cortex and end in the thalamus. From anatomy we know that such tracts start from each section of the M1/S1 strip and end at the VPL nucleus of the thalamus. Indeed, the TSS method found that most of these fibers end in close proximity to the VPL (within the 1–2 pixel border of it). We point out that the VPL was identified using the Talairach atlas coordinate system, which may vary from subject to subject, thus this result is satisfactory.

The two tracking algorithms (MP and RP) were tested on the pyramidal decussation region, which has two intersecting fiber systems: one going from the inferior to the superior direction and one going from the left to the right. Both algorithms were able to reproduce the inferior–superior decussation (see Fig. 6), but only the RP algorithm was able to adequately reconstruct the medial cerebellar peduncle fibers that cross in the left–right direction.

Future directions

One of the strengths of the combinatorial tracking method is that it discretesizes a PDF derived from DTI analysis (i.e. the ellipsoid). It has recently become clear that the DTI's ellipsoid is only a first order estimation of a Gaussian distribution of the anisotropic diffusion in the tissue. More advanced methodologies can now reproduce a more accurate PDF of the diffusion in tissue, taking into account restricted diffusion and compartmentalization issues. These more accurate PDFs can be plugged into our method and used for fiber-tracking.

One of the weaknesses of the method is that it does not take into consideration the uncertainty in the transition probability p_{ij}, which originates from its being statistically estimated. One possible solution is to formulate and solve a Stochastic Programming problem for the most probable random walk path. Another possible solution is to introduce a tensor field regularization prior to discretization, as done by Zhang and Hancock (2006). Zhang models the DTI image using a weighted graph, where the weights of edges are functions of the geodesic distances between tensors. Diffusion across this graph with time is captured by the heat equation, and the solution is found by exponentiation of the Laplace eigen system with time.

Combinatorial tracking should also be tested for the effects of noise since signal-to-noise ratio (SNR) is known to dramatically affect DTI and fiber-tracking. Poor SNR causes a more uniform distribution of the transition probability between adjacent voxels, reducing the probability of a specific path. Whether it is preferable to other paths in terms of the SNR requires further study.

Acknowledgments

The authors wish to thank the Ministry of Science and Technology of the State of Israel (the Tashtiot program) and the Israel Science Foundation (F.I.R.S.T. Bikura program) for the financial support. The authors also wish to thank Prof. Boris Tsirelson and Mr. Ofer Pasternak for their helpful discussions, and Ms. Efrat Sasson for the MRI data.

Appendix A. Markov Chain theory and the fundamental matrix theorem

A discrete time finite state Markov Chain (Durrett, 1999) is a stochastic process, defined by a finite set of states and by transition probability matrix **P**. At every discrete point in time the system may change state according to transition probability. The transition probability depends solely on the current state and not on any past state that the chain has visited in. A finite state Markov Chain can be described by a graph, where the weights associated with edges represent transition probabilities.

An irreducible Markov Chain is a chain in which there exists a path with non-zero probability from every state to every other state.

A stationary distribution π is a distribution of states such that $\pi^*\mathbf{P}=\pi$. For a finite irreducible Markov chain, a stationary distribution exists and it is unique (Durrett, 1999).

The stationary distribution π can be calculated by the solution of Eq. (A1). π is found by replacing any of the row vector of $(\mathbf{P}-\mathbf{I})^{\mathrm{T}}$ with a vector of "1" and the corresponding element in the right-hand side vector with one. This reflects the additional condition $\sum_i \pi(i) = 1$ (William, 2000).

$$\begin{aligned} &(\mathbf{P}-\mathbf{I})^T\pi^T = 0 \\ &\text{s.t.} \quad \textstyle\sum_i \pi(i) = 1 \end{aligned} \tag{A1}$$

A variant of this technique is the Grassmann, Taksar, and Heyman (GTH) algorithm (Grassmann et al., 1985), which is used in this work.

The recurrence time is defined as the time until return to state *i*. For a finite irreducible Markov chain the mean recurrence time is related to the stationary distribution by:

$$M_{ii} = \frac{1}{\pi(i)} \tag{A2}$$

For a finite irreducible Markov chain, the **M** matrix can be calculated by the following method, which employs the fundamental matrix theorem (Grinstead and Snell, 1997):

1) Construct **W**, a matrix whose rows are vector π.
2) Calculate the matrix $\mathbf{Z}=(\mathbf{I}-\mathbf{P}+\mathbf{W})^{-1}$.
3) Every element of **M** can be calculated by:

$$M_{ij} = \frac{z_{jj} - z_{ij}}{\pi(j)} \tag{A3}$$

where **I** is the identity matrix and **P** is the transition probability matrix. Note that the diagonal elements of **M** (mean recurrence time) are not calculated by this method.

References

Ahuja, R.K., Magnanti, T.L., Orlin, J.B., 1993. Network Flows: Theory, Algorithms, and Applications. Prentice Hall, Upper Saddle River, N.J. xv, 846 p.
Alexander, A.L., Hasan, K.M., Lazar, M., Tsuruda, J.S., Parker, D.L., 2001. Analysis of partial volume effects in diffusion-tensor MRI. Magn. Reson. Med. 45 (5), 770–780.
Assaf, Y., Pasternak, O., 2008. Diffusion tensor imaging (DTI)-based white matter mapping in brain research: a review. J. Mol. Neurosci. 34 (1), 51–61.
Assaf, Y., Ben-Sira, L., Constantini, S., Chang, L.C., Beni-Adani, L., 2006. Diffusion tensor imaging in hydrocephalus: initial experience. AJNR Am. J. Neuroradiol. 27 (8), 1717–1724.
Basser, P.J., Pierpaoli, C., 1998. A simplified method to measure the diffusion tensor from seven MR images. Magn. Reson. Med. 39 (6), 928–934.
Basser, P.J., Pajevic, S., Pierpaoli, C., Duda, J., Aldroubi, A., 2000. In vivo fiber tractography using DT-MRI data. Magn. Reson. Med. 44 (4), 625–632.
Behrens, T.E., Johansen-Berg, H., Woolrich, M.W., Smith, S.M., Wheeler-Kingshott, C.A., Boulby, P.A., Barker, G.J., Sillery, E.L., Sheehan, K., Ciccarelli, O., Thompson, A.J., Brady, J.M., Matthews, P.M., 2003a. Non-invasive mapping of connections between human thalamus and cortex using diffusion imaging. Nat. Neurosci. 6 (7), 750–757.
Behrens, T.E., Woolrich, M.W., Jenkinson, M., Johansen-Berg, H., Nunes, R.G., Clare, S., Matthews, P.M., Brady, J.M., Smith, S.M., 2003b. Characterization and propagation of uncertainty in diffusion-weighted MR imaging. Magn. Reson. Med. 50 (5), 1077–1088.
Catani, M., Howard, R.J., Pajevic, S., Jones, D.K., 2002. Virtual in vivo interactive dissection of white matter fasciculi in the human brain. NeuroImage 17 (1), 77–94.
Chou, M.C., Lin, Y.R., Huang, T.Y., Wang, C.Y., Chung, H.W., Juan, C.J., Chen, C.Y., 2005. FLAIR diffusion-tensor MR tractography: comparison of fiber tracking with conventional imaging. AJNR Am. J. Neuroradiol. 26 (3), 591–597.
Chung, F.R.K., 1997. Spectral Graph Theory. Am. Math. Soc., Providence, R.I. xi, 207 p.
Ciccarelli, O., Behrens, T.E., Altmann, D.R., Orrell, R.W., Howard, R.S., Johansen-Berg, H., Miller, D.H., Matthews, P.M., Thompson, A.J., 2006. Probabilistic diffusion

tractography: a potential tool to assess the rate of disease progression in amyotrophic lateral sclerosis. Brain 129 (Pt. 7), 1859–1871.
Conturo, T.E., Lori, N.F., Cull, T.S., Akbudak, E., Snyder, A.Z., Shimony, J.S., McKinstry, R.C., Burton, H., Raichle, M.E., 1999. Tracking neuronal fiber pathways in the living human brain. Proc. Natl. Acad. Sci. U. S. A. 96 (18), 10422–10427.
Durrett, R., 1999. Essentials of Stochastic Processes. Springer, New York. vi, 281 p.
Dyrby, T.B., Sogaard, L.V., Parker, G.J., Alexander, D.C., Lind, N.M., Baare, W.F., Hay-Schmidt, A., Eriksen, N., Pakkenberg, B., Paulson, O.B., Jelsing, J., 2007. Validation of in vitro probabilistic tractography. NeuroImage 37 (4), 1267–1277.
Fout, N., Huang, J., Z. D. Visualization of neuronal fiber connections from DT-MRI with global optimization. ACM Symposium on Applied Computing 2005:1200–1206.
Ge, Y., Law, M., Grossman, R.I., 2005. Applications of diffusion tensor MR imaging in multiple sclerosis. Ann. N.Y. Acad. Sci. 1064, 202–219.
Grassmann, W.K., Taksar, M.I., Heyman, D.P., 1985. Regenerative analysis and steady state distribution for Markov chains. Operat. Res. 33, 1107–1116.
Grinstead, C.M., Snell, J.L., 1997. Introduction to Probability. Am. Math. Soc., Providence, RI. xi, 510 p.
Huppi, P.S., Dubois, J., 2006. Diffusion tensor imaging of brain development. Semin. Fetal Neonatal Med. 11 (6), 489–497.
Iturria-Medina, Y., Canales-Rodriguez, E.J., Melie-Garcia, L., Valdes-Hernandez, P.A., Martinez-Montes, E., Aleman-Gomez, Y., Sanchez-Bornot, J.M., 2007. Characterizing brain anatomical connections using diffusion weighted MRI and graph theory. NeuroImage 36 (3), 645–660.
Jbabdi, S., Woolrich, M.W., Andersson, J.L., Behrens, T.E., 2007. A Bayesian framework for global tractography. NeuroImage 37 (1), 116–129.
Jones, D.K., 2003. Determining and visualizing uncertainty in estimates of fiber orientation from diffusion tensor MRI. Magn. Reson. Med. 49 (1), 7–12.
Jones, D.K., Pierpaoli, C., 2005. Confidence mapping in diffusion tensor magnetic resonance imaging tractography using a bootstrap approach. Magn. Reson. Med. 53 (5), 1143–1149.
Koch, M.A., Norris, D.G., Hund-Georgiadis, M., 2002. An investigation of functional and anatomical connectivity using magnetic resonance imaging. NeuroImage 16 (1), 241–250.
Lazar, M., Alexander, A.L., 2005. Bootstrap white matter tractography (BOOT-TRAC). NeuroImage 24 (2), 524–532.
Mori, S., Crain, B.J., Chacko, V.P., van Zijl, P.C., 1999. Three-dimensional tracking of axonal projections in the brain by magnetic resonance imaging. Ann. Neurol. 45 (2), 265–269.
Mukherjee, P., 2005. Diffusion tensor imaging and fiber tractography in acute stroke. Neuroimaging Clin. N. Am. 15 (3), 655–665 xii.
Mukherjee, P., McKinstry, R.C., 2006. Diffusion tensor imaging and tractography of human brain development. Neuroimaging Clin. N. Am. 16 (1), 19–43 vii.
Papadakis, N.G., Martin, K.M., Mustafa, M.H., Wilkinson, I.D., Griffiths, P.D., Huang, C.L., Woodruff, P.W., 2002. Study of the effect of CSF suppression on white matter diffusion anisotropy mapping of healthy human brain. Magn. Reson. Med. 48 (2), 394–398.
Park, S., Sener, M.K., Lu, D., Schulten, K., 2003. Reaction paths based on mean first-passage times. J. Chem. Phys. 119 (3), 7.
Parker, G.J., Haroon, H.A., Wheeler-Kingshott, C.A., 2003. A framework for a streamline-based probabilistic index of connectivity (PICo) using a structural interpretation of MRI diffusion measurements. J. Magn. Reson. Imaging 18 (2), 242–254.
Pierpaoli, C., Jezzard, P., Basser, P.J., Barnett, A., Di Chiro, G., 1996. Diffusion tensor MR imaging of the human brain. Radiology 201 (3), 637–648.
Poynton, C., Lal, R., Ratnanather, J.T., Mori, S., Boatman, D., Miller, M.I., Probabilistic tracking of fiber pathways using dynamic programming. 11th Annual Meeting of the Organization for Human Brain Mapping 2005.
Price, G., Cercignani, M., Parker, G.J., Altmann, D.R., Barnes, T.R., Barker, G.J., Joyce, E.M., Ron, M.A., 2008. White matter tracts in first-episode psychosis: a DTI tractography study of the uncinate fasciculus. NeuroImage 39 (3), 949–955.
Rollins, N.K., 2007. Clinical applications of diffusion tensor imaging and tractography in children. Pediatr. Radiol. 37 (8), 769–780.
Schonberg, T., Pianka, P., Hendler, T., Pasternak, O., Assaf, Y., 2006. Characterization of displaced white matter by brain tumors using combined DTI and fMRI. NeuroImage 30 (4), 1100–1111.
Sherbondy, A.J., Dougherty, R.F., Ben-Shachar, M., Napel, S., Wandell, B.A., 2008. ConTrack: finding the most likely pathways between brain regions using diffusion tractography. J. Vis. 8 (9), 11–16 15.
Siek, J.G., Lee, LQ, Lumsdaine, A., 2001. The Boost Graph Library: User Guide and Reference Manual. Addison-Wesley Professional, 352 p.
Whaley, R.C., Dongarra, J.J., Automatically tuned linear algebra software. Proc SC: High Performance Networking and Computing Conference 1998:1–27.
William, J.S., 2000. Numerical analysis methods. Performance Evaluation: Origins and Directions. Springer-Verlag.
Witwer, B.P., Moftakhar, R., Hasan, K.M., Deshmukh, P., Haughton, V., Field, A., Arfanakis, K., Noyes, J., Moritz, C.H., Meyerand, M.E., Rowley, H.A., Alexander, A.L., Badie, B., 2002. Diffusion-tensor imaging of white matter tracts in patients with cerebral neoplasm. J. Neurosurg. 97 (3), 568–575.
Zhang, F., Hancock, E.R., 2006. Riemannian graph diffusion for DT-MRI regularization. Med. Image Comput. Comput. Assist. Interv. Int. Conf. Med. Image Comput. Comput Assist. Interv. 9 (Pt. 2), 234–242.
Zhang, F., Hancock, E.R., Goodlett, C., Gerig, G., 2009. Probabilistic white matter fiber tracking using particle filtering and von Mises–Fisher sampling. Med. Image Anal. 13 (1), 5–18.